Resource and Trajectory Optimization for UAV-Relay-Assisted Secure Maritime MEC

Fangwei Lu, Gongliang Liu, Weidang Lu, *Senior Member, IEEE*, Yuan Gao, Jiang Cao, Nan Zhao, *Senior Member, IEEE*, Arumugam Nallanathan, *Fellow, IEEE*

***Abstract*—With the evolutional development of maritime networks, the explosive growth of maritime data has put forward elevated demands for the computing capabilities of maritime devices (MDs). Unmanned aerial vehicle (UAV) is able to alleviate the computing pressure of MDs by forwarding the computing tasks to the edge server on the coast. However, UAV relaying introduces a significant security challenge due to the vulnerability of line-of-sight (LoS) communication channels, which can be exploited for eavesdropping on computing tasks. In this paper, an efficient secure communication scheme is proposed for UAV-relay-assisted maritime mobile edge computing (MEC) with a flying eavesdropper. The secure computing capacity of MDs is maximized by jointly optimizing the transmit power, time slot allocation factor, computation optimization and UAV trajectory. Due to multi-variable coupling, the formulated optimization problem (OP) is non-convex. We first transform OP by introducing auxiliary variables. Then, the transformed OP is decomposed and solved in an iterative manner by applying block coordinate descent (BCD) and successive convex approximation (SCA). Numerical results show that the secure computing capability of the UAV-relay-assisted maritime MEC system of proposed secure communication scheme can be effectively improved compared with benchmarks.**

***Index Terms*—Secure transmission, MEC, UAV-relay, maritime communications.**

I. Introduction

With the evolutional development of technological advancements, the maritime services are becoming more and more important, e.g., maritime fishery, transportation, search and rescue, and military activities. To better realize miscellaneous maritime services, it is urgent to establish reliable links between maritime devices (MDs) and the coast [1]. The explosive growth of massive maritime data will put forward higher requirements for the computing capabilities of MDs [2]. Through offloading the computation tasks to the edge servers with more powerful capability deployed on the coast, mobile edge computing (MEC) has the capability to effectively alleviate the computation pressure of MDs [3]. However, most of MDs are deployed far from the coast. Limited by the maritime infrastructure and poor maritime channels, the direct communication between MDs and the coastal edge server (CES) is always difficult to support the transmission of massive computing tasks.

Taking advantage of the inherent characteristics of high mobility and flexibility [4], [5], unmanned aerial vehicles (UAVs) can be utilized to enhance the transmission quality between MDs and CES by serving as a mobile relay [6]. Through the optimization of both relay trajectory and power, Zeng *et al.* utilized the controllable channel changes caused by relay movement under the constraints of UAV movement and information causality, leading to an improvement in end-to-end throughput [7]. Chen *et al.* analyzed the interrupt performance and bit error rate of single and multi-hop links in multiple UAVs relaying systems through designing the optimal placement of UAVs [8]. In [9], Zhao *et al.* presented a framework that utilizes UAVs to establish information exchange via multi-hop UAV relaying. Zhong *et al.* in [10] handled uncertain channel models and communication node locations for the UAV-assisted-relaying networks. Liang *et al.* investigated a UAV-assisted bidirectional relaying scheme that involved multiple ground user pairs [11]. Zhang *et al.* utilized UAV-assisted decode-and-forward relaying by adjusting placement of the UAV to enhance the caching performance [12]. Zhan *et al.* minimized the completion time and energy consumption of the UAV-enabled MEC system by jointly designing the computation offloading, resource allocation and UAV trajectory [13].

With the assistance of UAV relaying, the flexibility of MEC can be enhanced [14]. Specifically, UAV can facilitate the offloading of computing tasks to the CES that possesses superior computational capabilities [15]. Hu *et al.* studied the effectiveness of UAV-assisted MEC with various constraints, such as task bandwidth allocation, information causality, and UAV trajectory [16]. Liu *et al.* maximized the energy-efficiency of the maritime system by jointly optimizing the UAV's trajectory and the individual transmit power levels of the source and the UAV relay nodes [17]. Na *et al.* investigated a high-efficiency scheme for UAV relaying communication maritime system with the UAV trajectory and resource allocation optimization [18]. Zhang and Ansari jointly optimized the UAV deployment, terminal association, time allocation of access and backhaul links, computing resource distribution to minimize the average delay of terminals, with UAVs serving as computing and relaying nodes [19]. Liu *et al.* investigated a multi-input single-output UAV-assisted MEC scheme that

Fangwei Lu and Gongliang Liu are with the Department of Communication Engineering, Harbin Institute of Technology, Weihai 264209, China (e-mail: lufangwei2022@163.com; liugl@hit.edu.cn).

Weidang Lu is with the College of Information Engineering, Zhejiang University of Technology, Hangzhou 310023, China (e-mail: luweid@zjut.edu.cn).

Yuan Gao and Jiang Cao are with the Academy of Military Science of the PLA, China (e-mail: yuangao08@tsinghua.edu.cn; caojiangjk@outlook.com).

Nan Zhao is with the School of Information and Communication Engineering, Dalian University of Technology, Dalian 116024, P. R. China (e-mail: zhaonan@dlut.edu.cn).

Arumugam Nallanathan is with School of Electronic Engineering and Computer Science, Queen Mary University of London, E1 4NS, U.K. (e-mail: a.nallanathan@qmul.ac.uk).

addressed the challenges of poor channel quality due to multi-path and blocking in traditional MEC networks [20]. He *et al.* in [21] proposed a scheme for multi-hop task offloading based on dynamic computing that aimed to achieve more powerful remote edge computing using multiple UAVs. Zhao *et al.* in [22] presented an optimization framework that involves UAV-assisted vehicle computing and offloading, in which the offloading decision problem was transformed into a multi-player computational offloading sequence game problem.

Nevertheless, due to the line-of-sight (LoS) characteristics, the offloaded data of UAV-assisted MEC networks can be easily eavesdropped, causing serious security threat [23]. Physical layer security enables the achievement of secure offloading, protecting the data against malicious eavesdropping [24], [25]. Wang *et al.* investigated transmission optimization in a four-node system with the goal of maximizing the secure rate, and proposed an iterative algorithm based on the difference-of-concave method [26]. Zhou *et al.* conducted a joint secure transmission optimization of UAV position, computing power, user association, transmit power and offloading ratio with multiple eavesdropping UAVs [27]. Li *et al.* investigated a energy-saving scheme for UAV-MEC secure transmissions, where the optimization of transmit power, task allocation, and UAV placement was performed with considering secure offloading rate constraints [28]. Xu *et al.* employed a two-UAV framework to facilitate secure transmissions with the existence of multiple ground eavesdroppers, where one UAV was utilized for offloading tasks, while the other was dedicated to mitigating the risk of malicious eavesdropping [29]. Meanwhile, a secure computation scheme was investigated by Lu *et al.* to overcome the secure threat in UAV-assisted MEC, where one UAV offering computing services to the users and another UAV eavesdropping on the transmission of their data [30], [31]. Comparing with the ground eavesdroppers, which are deployed at the fixed positions in the existing works, UAV eavesdroppers will have much better channel condition. Thus, the information can be easily eavesdropped by flying UAVs. The major challenges for considering UAV eavesdroppers are to consider the anti-collision constraint between UAVs, which is not considered for ground eavesdroppers.

However, the secure transmission in UAV-relay-assisted maritime MEC has not been well studied in existing works. Thus, an effective secure communication scheme is proposed in this paper for the UAV-relay-assisted maritime MEC network. Specifically, a UAV relay (UAV_r) helps MDs offload tasks to a CES, while a UAV eavesdropper (UAV_e) eavesdrops the offloaded data. To prevent eavesdropping, a coastal jammer (CJ) generates the jamming signals to disrupt UAV_e eavesdropping. UAV_r trajectory, time slot allocation, transmit power and computing assignment are optimized to maximize the minimum secure computing capacity of MDs. The contributions are summarized as follows.

- Due to the LoS transmission, the secure transmission remains as a challenging issue in UAV-relay assisted maritime MEC networks, which has not been well studied in the existing works. Thus, we propose a secure communication scheme for UAV-relay-assisted maritime MEC networks.

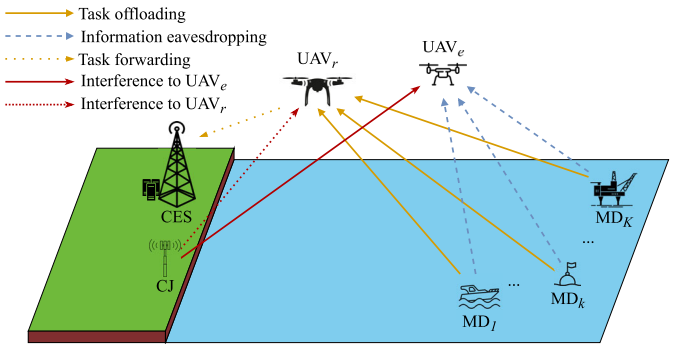

Fig. 1. UAV-relay-assisted secure maritime MEC system.

- In the proposed scheme, UAV_r helps MDs to offload computing tasks to CES. CJ emits the jamming signals to disrupt UAV_e eavesdropping. Considering the constraints of the flight speed and anti-collision of UAV, the transmit power of MDs and UAV_r, the local computing capacity of MDs, an optimization problem (OP) is formulated to maximize the minimum secure computing capacity by optimizing the transmit power, time slot allocation factor, computation allocation and UAV trajectory.
- To tackle this multivariate coupling OP, a block coordinate descent (BCD) based joint optimization algorithm is proposed. Specifically, we first introduce auxiliary variables to facilitate the transformation of OP into an equivalent form. Subsequently, OP is decomposed into a set of subproblems. Then, based on SCA, the approximate solution is efficiently obtained in an iterative way. Furthermore, the feasibility and complexity of the proposed scheme are discussed to prove the effectiveness.

The rest of the paper is organized as follows. The UAV-relay-assisted secure maritime MEC system is introduced in Section II. Section III formulates the problem of maximizing secure computing capacity. A BCD-based joint optimization algorithm is studied in Section IV to solve OP. Numerical results are shown and analyzed in Section V. Section VI concludes the paper.

II. System Model

A UAV-relay-assisted secure maritime MEC system is considered as shown in Fig. 1. There are K MDs, two UAVs (UAV_r and UAV_e), one CES and one CJ. UAV_r forwards the computing tasks of MDs to CES through amplify-and-forward (AF) relaying. UAV_e eavesdrops the transmission from MDs to UAV_r. CJ sends the jamming signal to disrupt the eavesdropping. We assume that CES has prior knowledge of the jamming signal sent by CJ because CES and CJ belong to the legitimate network, the jamming signal sent by CJ are friendly to CES. Thus, CES will not be affected by the artificial jamming signals. However, UAV_e is unaware of CJ's presence because UAV_e is a mobile eavesdropper and it does not belong to the legitimate network. We assume that UAV_r and CES already know the channel state information among CES, CJ, UAV_r and MDs in advance by means of synthetic aperture radar, etc. The symbols used are shown in Table I.

TABLE I
NOTATIONS

Notation	Description
$\mathbf{v}_k$	Location of MD$_k$
$\mathbf{v}_s$	Location of CES
$\mathbf{v}_j$	Location of CJ
$\mathbf{u}_i[n]$	Location of UAV$_i$
H_i	Altitude of UAV$_i$
φ_t	Length of the time slot
T	Flight period of UAVs
N	Number of total time slots
$\mathbf{u}_i^I$	Initial position of UAV$_i$
$\mathbf{u}_i^F$	Final position of UAV$_i$
$V_i^{\max}$	Maximum speed of UAV$_i$
$d_{\min}$	Minimum distance between UAVs
$\widetilde{G}[n]$	Power ratio of the signal
β_0	Channel power gain at a unit distance
$P_k^{\max}$	Peak power of MD$_k$
$P_r^{\max}$	Peak power of UAV$_r$
$p_k[n]$	Transmit power of MD$_k$
$p_r[n]$	Transmit power of UAV$_r$
$\xi_k[n]$	Time slot allocation factor
$x_k[n]$	Transmit signal of MD$_k$
$x_j[n]$	Transmit signal of CJ
n_r	Noise power of UAV$_r$
n_e	Noise power of UAV$_e$
n_s	Noise power of CES
c_k	CPU cycles for MD calculating per bit
c_s	CPU cycles for CES calculating per bit
$l_{k,\mathrm{loc}}[n]$	Local computing allocation of MD$_k$
$F_k^{\max}$	Peak CPU frequency of MD
$F_s^{\max}$	Peak CPU frequency of CES
W	Communication bandwidth
Q_k	Secure computing requirement of MD$_k$
k_k	CPU capacity coefficient of MDs
P_k^{ave}	Power budge of MD$_k$

The horizontal coordinates of MD$_k$, CES and CJ are described as $\mathbf{v}_{u_0} = (x_{u_0}, y_{u_0})^T, u_0 \in \{k, s, j\}$, where $k \in \mathcal{K} = \{1, 2, \ldots, K\}$. The flight period of UAVs is given by $T, T \geq 0$. The position of UAV$_i$ at time t is denoted as $\mathbf{u}_i(t), i \in \{r, e\}, t \in [0, T]$. Assume that the altitude of UAV$_i$ is constant, denoted by H_i. To simplify the discussion, T is uniformly partitioned into N discrete time slots. Thus, the length of a single slot is $\varphi_t = T/N$. In slot n, the position of UAV$_i$ is denoted as $\mathbf{u}_i[n] = (x_i[n], y_i[n])^T$.

Assume that UAV$_i$ flies from the setting initial position $\mathbf{u}_i^I$ to the setting final position $\mathbf{u}_i^F$ within the period T. The flight speed of UAV$_r$ cannot exceed $V_r^{\max}$. Then, the maximum allowable displacement of UAV$_r$ in a single time slot is $l_r^{\max} = V_r^{\max}\varphi_t$. Then, we have

$$\mathbf{u}_r[1] = \mathbf{u}_r^I, \tag{1a}$$

$$\mathbf{u}_r[N] = \mathbf{u}_r^F, \tag{1b}$$

$$\|\mathbf{u}_r[n+1] - \mathbf{u}_r[n]\| \leq l_r^{\max}. \tag{1c}$$

To avoid collision of UAV$_r$ and UAV$_e$, the minimum collision avoidance distance between them is $d_{\min}$. We have

$$\|\mathbf{u}_r[n] - \mathbf{u}_e[n]\|^2 \geq d_{\min}^2. \tag{2}$$

In this work, we use distance-dependent path loss model [29]. In slot n, the distances between MD$_k$ and UAV$_r$, MD$_k$ and UAV$_e$, CJ and UAV$_r$, CJ and UAV$_e$, UAV$_r$ and CES can be respectively expressed as

$$d_{u_1,u_2}[n] = \sqrt{H_{u_2}^2 + \|\mathbf{u}_{u_2} - \mathbf{v}_{u_1}\|^2}, \tag{3}$$

where $(u_1, u_2) \in \{(k, r), (k, e), (j, r), (j, e), (s, r)\}$.

Since CES and CJ are deployed on the coast, we consider them to be approximated as maritime nodes. Thus, the channels between MD$_k$ and UAV$_r$, MD$_k$ and UAV$_e$, CJ and UAV$_r$, CJ and UAV$_e$, UAV$_r$ and CES can be considered as air-to-sea channels. They follow Rician fading, which can be taken as composite channels of large-scale fading and small-scale fading [32], [33]. Thus, the corresponding channel coefficients can be expressed as

$$\begin{aligned} h_{u_1,u_2}[n] &= g_{u_1,u_2}[n]\widetilde{h}_{u_1,u_2}[n] \\ &= \sqrt{\frac{\beta_0}{d_{u_1,u_2}^2[n]}}\left(\sqrt{\frac{\widetilde{G}[n]}{\widetilde{G}[n]+1}} + \sqrt{\frac{1}{\widetilde{G}[n]+1}}\widetilde{g}_{u_1,u_2}[n]\right)^2, \end{aligned} \tag{4}$$

where $\{g_{u_1,u_2}[n]\}$ and $\{\widetilde{h}_{u_1,u_2}[n]\}$ are the large-scale fading coefficients and small-scale fading coefficients, respectively. β_0 is channel power gain at a unit distance on the LoS component of the signal, and $\widetilde{G}[n]$ is the power ratio of the LoS to the non-line-of-sight (NLoS) signal. $\widetilde{g}_{u_1,u_2}[n] \in \mathcal{CN}(0, 1)$ is the ratio of the NLoS component matrix between the LoS component matrix of the signal.

Define $P_k^{\max}$ and $P_r^{\max}$ as the peak power of MD$_k$ and UAV$_r$, respectively. The transmit power of MD$_k$ and UAV$_r$ need to satisfy

$$0 \leq p_k[n] \leq P_k^{\max}, \forall k, n, \tag{5a}$$

$$0 \leq p_r[n] \leq P_r^{\max}, \forall k, n. \tag{5b}$$

III. Problem Formulation

In the previous section, the flight period T is uniformly partitioned into N discrete time slots based on the flight trajectory of UAVs. In each slot, every MD can access the UAV$_r$ for task forwarding and offloading. To avoid the communication interference between MDs, task offloading is performed using time-division-multiple-access, where one slot is further partitioned into K subslots. The length of time allocated to MD$_k$ is $\xi_k[n]\varphi_t$, where $\xi_k[n]$ is time slot allocation factor. $\xi_k[n]$ is limited by

$$\sum_{k=1}^{K} \xi_k[n] \leq 1, \forall n, \tag{6a}$$

$$0 \leq \xi_k[n] \leq 1, \forall k, n. \tag{6b}$$

A. Communication Model

Each subslot $\xi_k[n]\varphi_t$ is further divided into two phases with equal length of time.

In the first phase, MD$_k$ offloads its computing task to UAV$_r$, which will be eavesdropped by UAV$_e$. CJ transmits signals to interfere the eavesdropping of UAV$_e$. Thus, the signal received in the first phase of UAV$_r$ is

$$y_{k,r}^{(1)}[n] = \sqrt{p_k[n]}h_{k,r}[n]x_k[n] + \sqrt{P_j}h_{j,r}[n]x_j[n] + n_r, \forall k, n, \tag{7}$$

$$\gamma_{k,s}[n]=\frac{p_k[n]|h_{k,r}[n]|^2p_r[n]|h_{r,s}[n]|^2}{p_r[n]|h_{r,s}[n]|^2n_r^2+p_k[n]|h_{k,r}[n]|^2n_s^2+P_j|h_{j,r}[n]|^2n_s^2+n_r^2n_s^2},\forall k,n. \quad (13)$$

where P_j is the transmit power of CJ, $x_k[n]$ and $x_j[n]$ is the information sent by MD_k and CJ, respectively, and n_r is the received noise of UAV_r.

Assume that $x_k[n]$ and $x_k[j]$ are both normalized,

$$\mathbb{E}\{\|x_k[n]\|^2\}=\mathbb{E}\{\|x_j[n]\|^2\}=1,\forall n. \quad (8)$$

When UAV_e eavesdrops the transmission from MD_k to UAV_r in the first phase, it also receives the interfering signal transmitted by CJ. Thus, the signal received by UAV_e is

$$y_{k,e}^{(1)}[n]=\sqrt{p_k[n]}h_{k,e}[n]x_k[n]+\sqrt{P_j}h_{j,e}x_j[n]+n_e,\forall k,n, \quad (9)$$

where n_e is the received noise of UAV_e.

As UAV_e cannot distinguish the interfering signal transmitted by CJ, the SINR of UAV_e eavesdropping on the signal from MD_k to UAV_r can be expressed as

$$\gamma_{k,e}[n]=\frac{|h_{k,e}[n]|^2p_k[n]}{|h_{j,e}[n]|^2P_j+n_e^2},\forall k,n. \quad (10)$$

In the second phase, UAV_r forwards the information to CES via AF. The amplification factor is

$$G_{k,r}[n]=\sqrt{\frac{p_r[n]}{|h_{k,r}[n]|^2p_k[n]+|h_{j,r}[n]|^2P_j+n_r^2}},\forall k,n, \quad (11)$$

where $p_r[n]$ is UAV_r's transmit power.

Then, the signal received by CES is

$$y_{r,s}^{(2)}[n]=G_{k,r}[n]h_{r,s}[n]y_{k,r}^{(1)}[n]+n_s, \quad (12)$$

where n_s is the received noise of CES.

Since CES knows the interfering signal of CJ in advance, the SINR of CES from MD_k is written as (13).

Therefore, the task offloading rate from MD_k to CES is

$$\Phi_{k,s}[n]=\log_2\left(1+\gamma_{k,s}[n]\right),\forall k,n. \quad (14)$$

The eavesdropping rate from MD_k to UAV_e is

$$\Phi_{k,e}[n]=\log_2\left(1+\gamma_{k,e}[n]\right),\forall k,n. \quad (15)$$

Then, the secure offloading rate from MD_k to CES is

$$\Phi_{k,\mathrm{sec}}[n]\triangleq\left(\Phi_{k,s}[n]-\Phi_{k,e}[n]\right)^+. \quad (16)$$

B. Computing Model

A partial offload strategy is adopted at MDs, in which, a part of tasks are executed on MDs, and the other tasks are forwarded to CES through UAV_r for execution.

Assume that the number of CPU cycles for MD_k when calculating a single bit data are c_k. The amount of data computed locally by MD_k in slot n are $l_{k,\mathrm{loc}}[n]$. Assume that MD_k's maximum CPU frequency is $F_k^{\max}$. Thus, we have

$$c_kl_{k,\mathrm{loc}}[n]\le\varphi_tF_k^{\max},\forall k,n. \quad (17)$$

Define the CPU cycles of CES to calculate a single bit data as c_s, and CES's maximum CPU frequency as $F_s^{\max}$. Thus, the number of bits computed on CES cannot exceed its computing capacity, satisfying

$$\frac{1}{2}c_sW\xi_k[n]\varphi_t\Phi_{k,\mathrm{sec}}[n]\le\frac{1}{2}\varphi_t\xi_k[n]F_s^{\max}, \quad (18)$$

where W is bandwidth.

Define the minimum secure computing requirement of MD_k as Q_k. To guarantee the secure computing requirement of each MD, we have

$$l_{k,\mathrm{loc}}[n]+\frac{1}{2}W\xi_k[n]\varphi_t\Phi_{k,\mathrm{sec}}[n]\ge Q_k,\forall k,n. \quad (19)$$

If tasks are computed locally at MD_k, the energy consumption can be written as

$$E_{k,\mathrm{loc}}[n]=\frac{k_k\left(c_kl_{k,\mathrm{loc}}[n]\right)^3}{\varphi_t^2}, \quad (20)$$

where k_k denotes the effective capacitance coefficient of MD_k.

On the other hand, if tasks are computed remotely at CES, the energy of MD_k is consumed at transmitting

$$E_{k,\mathrm{trans}}[n]=\frac{1}{2}\xi_k[n]\varphi_tp_k[n]. \quad (21)$$

The energy consumption of MD_k in the whole period T should satisfy

$$\frac{1}{T}\sum_{n=1}^{N}\left(E_{k,\mathrm{loc}}[n]+E_{k,\mathrm{trans}}[n]\right)\le P_k^{\mathrm{ave}},\forall k, \quad (22)$$

where P_k^{ave} is the average power limit of MD_k.

C. Problem Formulation

The secure computing capacity of MD_k is defined as the average number of bits that MD_k can achieve, which is composed of local and offloading computation,

$$\overline{\Phi}_{k,\mathrm{sec}}\triangleq\frac{1}{T}\left(\frac{1}{2}W\varphi_t\sum_{n=1}^{N}\xi_k[n]\Phi_{k,\mathrm{sec}}[n]+\sum_{n=1}^{N}l_{k,\mathrm{loc}}[n]\right),\forall k. \quad (23)$$

Our optimization target is to maximize the minimum secure computing capacity of the system by optimizing the time slot allocation factor $\xi_k[n]$, MD_k transmit power $p_k[n]$, UAV_r transmit power $p_r[n]$, the amount of data computed at MD_k locally $l_{k,\mathrm{loc}}[n]$ and the UAV_r trajectory $\mathbf{u}_r[n]$, which can be formulated as

$$\begin{aligned}(\mathrm{P1}):\ &\max_{\{\xi_k[n],p_k[n],p_r[n],l_{k,\mathrm{loc}}[n],\mathbf{u}_r[n]\}}\ \min_{\forall k}\overline{\Phi}_{k,\mathrm{sec}}\\ &\text{s.t. (1),(2),(5),(6),(17)-(22),}\end{aligned} \quad (24)$$

Due to coupling of multi-variables, non-convexity of constraints (2), (18), (19) and (22), (P1) is non-convex. Specifically, constraint (2) is non-convex. Constraints (18) and (19) are related to $\Phi_{k,\mathrm{sec}}[n]$, which is composed of multiple optimization variables, e.g., $p_k[n]$, $p_r[n]$, $\mathbf{u}_r[n]$, making (18) and (19) multi-variable coupled and non-convex. Moreover, the constraint (22) is also related to multiple optimization variables, e.g., $\xi_k[n]$, $p_k[n]$, $l_{k,\mathrm{loc}}[n]$, making (22) non-convex.

IV. Problem Solution

To simplify the resolution of the problem (1), we transform it into an equality form with three auxiliary variables θ, $\theta_{1,k}[n]$ and $\theta_{2,k}[n]$

$$\text{(P2)}: \max_{\mathcal{Z}} \theta \tag{25a}$$

$$\text{s.t. (1),(2),(5),(6),(17),(22),}$$

$$\theta \le \frac{1}{T}\left(\frac{1}{2}W\varphi_t \sum_{n=1}^{N} \xi_k[n]\left(\theta_{1,k}[n]-\theta_{2,k}[n]\right) + \sum_{n=1}^{N} l_{k,\mathrm{loc}}[n]\right), \forall k, \tag{25b}$$

$$\theta_{1,k}[n] \le \Phi_{k,s}[n], \forall k, n, \tag{25c}$$

$$\theta_{2,k}[n] \ge \Phi_{k,e}[n], \forall k, n, \tag{25d}$$

$$c_s W\left(\theta_{1,k}[n]-\theta_{2,k}[n]\right) \le F_s^{\max}, \forall k, n, \tag{25e}$$

$$l_{k,\mathrm{loc}}[n]+\frac{1}{2}B\xi_k[n]\varphi_t\left(\theta_{1,k}[n]-\theta_{2,k}[n]\right) \ge Q_k, \forall k, n, \tag{25f}$$

where $\mathcal{Z}=\{\xi_k[n], p_k[n], p_r[n], l_{k,\mathrm{loc}}[n], \mathbf{u}_r[n], \theta_{1,k}[n], \theta_{2,k}[n]\}$.

For (18), (19) and (23), by setting $p_k[n]=0$, $p_r[n]=0$ and $l_{k,\mathrm{loc}}[n]=0$, at least the value of zero can be obtained. Thus, we can omit the operator $[\cdot]^+$. We introduce the auxiliary variable s as the lower bound of $\overline{\Phi}_{k,\mathrm{sec}}$ as shown in (25b). Meanwhile, $\theta_{1,k}[n]$ is introduced to represent the lower bound of $\Phi_{k,s}[n]$ and $\theta_{2,k}[n]$ is introduced to represent the upper bound of $\Phi_{k,e}[n]$, as shown in (25c) and (25d), respectively. The value of θ can be always enlarged, unless the equality in (25b) is hold at the optimal solution. Similarly, in order to achieve the optimal solution, it is necessary for at least one equality in equations (25c) and (25e) to hold, thereby ensuring the same value as the problem (P1). Therefore, in the case of $\theta_{2,k}[n]$, the equality $\theta_{2,k}[n]=\max\Phi_{k,e}[n]$ must hold at the optimal solution. Otherwise, if $\theta_{2,k}[n]$ is not equal to $\max\Phi_{k,e}[n]$, it can always be decreased, leading to a larger value of the objective function. Therefore, the transformed problem (P2) is equivalent to (P1).

To overcome the problem (P2), a BCD-based joint optimization algorithm is proposed. We adopt a two-step approach with block structures of the variables. In Step 1, the variables $\mathcal{Z}\backslash\mathbf{u}_r[n]$ are optimized by considering $\mathbf{u}_r[n]$ at a fixed value. Subsequently, in Step 2, the variables $\mathbf{u}_r[n]$ is optimized by considering $\mathcal{Z}\backslash\mathbf{u}_r[n]$ fixed.

A. Step 1: Optimizing $\mathcal{Z}\backslash\mathbf{u}_r[n]$

For fixed $\mathbf{u}_r[n]$, the problem (P2) can be re-expressed as

$$\text{(P3)}: \max_{\mathcal{Z}} \theta \tag{26}$$
$$\text{s.t. (5),(6),(17),(22),(25b)-(25f).}$$

The problem (P3) has non-convex constraints, which are shown as (22),(25b)-(25d), and(25f). As a result, the problem (P3) is also non-convex. To overcome this non-convexity, we can utilize the BCD to solve [34]. Specifically, we can obtain the time slot allocation factor of MD$_k$ $\xi_k[n]$, MD$_k$ transmit power $p_k[n]$, UAV$_r$ transmit power $p_r[n]$, and MD$_k$ local computation allocation $l_{k,\mathrm{loc}}[n]$ by fixing the other values in an iterative manner.

1) Time Allocation: For the fixed MD$_k$ transmit power $p_k[n]$, UAV$_r$ transmit power $p_r[n]$ and MD$_k$ local computation allocation $l_{k,\mathrm{loc}}[n]$, the OP (P3) is

$$\text{(P3.1)}: \max_{\{\xi_k[n],\theta_{1,k}[n],\theta_{2,k}[n]\}} \theta \tag{27}$$
$$\text{s.t. (6),(22),(25b)-(25f).}$$

(P3.1) is a typical convex OP, which is solved using traditional convex optimization methods such as CVX [35].

2) MD$_k$ Transmit Power: For the fixed time slot allocation factor $\xi_k[n]$, UAV$_r$ transmit power $p_r[n]$ and MD$_k$ local computation allocation $l_{k,\mathrm{loc}}[n]$, the OP (P3) is formulated as

$$\text{(P3.2)}: \max_{\{p_k[n],\theta_{1,k}[n],\theta_{2,k}[n]\}} \theta \tag{28}$$
$$\text{s.t. (5a),(22),(25b)-(25f).}$$

Because of (25c) and (25d)'s non-convexity, (P3.2) is difficult to solve. The OP (P3.2) can be solved by SCA [36], where problem (P3.2) can be approximated as the convex problem in each iteration. The transmit power of MD$_k$ is obtained via iterations.

Assume that $p_k^{(i)}[n]$ is the value of the ith iteration of the transmit power $p_k[n]$ of MD$_k$. By applying SCA, we take the first-order Taylor expansion at the given $p_k^{(i)}[n]$, and convert (25c) to

$$\theta_{1,k}[n] \le \log_2\left(1+\frac{a_1 p_k^{(i)}[n]}{b_1 p_k^{(i)}[n]+c_1}\right) + \frac{a_1 c_1}{\ln 2}\frac{p_k[n]-p_k^{(i)}[n]}{\left(\left(a_1+b_1\right)p_k^{(i)}[n]+c_1\right)\left(b_1 p_k^{(i)}[n]+c_1\right)}, \tag{29}$$

where

$$\begin{cases} a_1 = |h_{k,r}[n]|^2 p_r[n]|h_{r,s}[n]|^2, \\ b_1 = |h_{k,r}[n]|^2 n_s^2, \\ c_1 = p_r[n]|h_{r,s}[n]|^2 n_r^2 + P_j|h_{j,r}[n]|^2 n_s^2 + n_r^2 n_s^2. \end{cases} \tag{30}$$

(25d) can be similarly converted to

$$\theta_{2,k}[n] \ge \log_2\left(1+\frac{a_2 p_k^{(i)}[n]}{b_2}\right)+\frac{a_2}{\ln 2}\frac{p_k[n]-p_k^{(i)}[n]}{a_2 p_k^{(i)}[n]+b_2}, \forall k,n, \tag{31}$$

where

$$\begin{cases} a_2 = |h_{k,e}[n]|^2, \\ b_2 = |h_{j,e}[n]|^2 P_j + n_e^2. \end{cases} \tag{32}$$

Thus, the problem (P3.2) can be reformulated as

$$\text{(P3.2.1)}: \max_{\{p_k[n],\theta_{1,k}[n],\theta_{2,k}[n]\}} \theta \tag{33}$$
$$\text{s.t. (5a),(22),(25b),(25e),(25f),(29),(31).}$$

Note that (P3.2.1) is convex, which can be solved through CVX.

3) UAV$_r$ Transmit Power: For the fixed time slot allocation factor $\xi_k[n]$, MD$_k$ transmit power $p_k[n]$ and MD$_k$ local computation allocation $l_{k,\mathrm{loc}}[n]$, the OP (P3) can be formulated as

$$\text{(P3.3)}: \max_{\{p_r[n],\theta_{1,k}[n],\theta_{2,k}[n]\}} \theta \quad \text{s.t. (5b),(25b)-(25f).} \tag{34}$$

The problem (P3.3) is difficult to solve as (25c) is non-convex. Similarly, we can use SCA to solve it. Assume that $p_r^{(i)}[n]$ is the value of the i_{th} iteration of the transmit power $p_r[n]$ of UAV$_r$. With the given point $p_r^{(i)}[n]$, through taking the first-order of Taylor expansion, we can convert (25c) as

$$\begin{aligned}\theta_{1,k}[n] \le \log_2\left(1+\frac{a_3 p_r^{(i)}[n]}{b_3 p_r^{(i)}[n]+c_3}\right) \\ + \frac{a_3 c_3}{\ln 2}\frac{p_r[n]-p_r^{(i)}[n]}{\left((a_3+b_3)\,p_r^{(i)}[n]+c_3\right)\left(b_3 p_r^{(i)}[n]+c_3\right)}, \forall k,n,\end{aligned} \tag{35}$$

where

$$\begin{cases} a_3 = p_k[n]|h_{k,r}[n]|^2|h_{r,s}[n]|^2, \\ b_3 = |h_{r,s}[n]|^2 n_r^2, \\ c_3 = p_k[n]|h_{k,r}[n]|^2 n_s^2 + P_j|h_{j,r}[n]|^2 n_s^2 + n_r^2 n_s^2. \end{cases} \tag{36}$$

Then, the problem (P3.3) can be reformulated as

$$\text{(P3.3.1)}: \max_{\{p_r[n],\theta_{1,k}[n],\theta_{2,k}[n]\}} \theta \quad \text{s.t. (5b),(25b),(25d)-(25f),(35).} \tag{37}$$

The constraints of the problem (P3.3.1) are all linear. Thus, the problem (P3.3.1) is typically convex, which can be solved by CVX.

4) MD$_k$ Local computation Allocation: For the fixed time slot allocation factor $\xi_k[n]$, MD$_k$ transmit power $p_k[n]$ and UAV$_r$ transmit power $p_r[n]$, the OP (P3) can be formulated as

$$\text{(P3.4)}: \max_{\{l_{k,\mathrm{loc}}[n],\theta_{1,k}[n],\theta_{2,k}[n]\}} \theta \quad \text{s.t. (17),(22),(25b)-(25f).} \tag{38}$$

As the constraint (22) is convex, and the rest constraints are linear, (P3.4) can be solved by CVX.

B. Step 2: Optimizing $\mathbf{u}_r[n]$

By fixing the time slot allocation factor $\xi_k[n]$, MD$_k$ transmit power $p_k[n]$, UAV$_r$ transmit power $p_r[n]$, and MD$_k$ local computation allocation $lk,\mathrm{loc}[n]$, we can reformulat the problem (P2) as

$$\text{(P4)}: \max_{\{\mathbf{u}_r[n],\theta_{1,k}[n],\theta_{2,k}[n]\}} \theta \quad \text{s.t. (1),(2),(25b)-(25f),} \tag{39}$$

where the constraints (2) and (25c) are non-convex.

Similarly, we can use SCA to solve it. Assume that $\mathbf{u}_r^{(i)}[n]$ is the value of the i_{th} iteration of the trajectory of UAV$_r$, through taking the first-order Taylor expansion, (2) and (25c) are converted to

$$\begin{aligned}&\|\mathbf{u}_r^{(i)}[n]-\mathbf{u}_e[n]\|^2 \\ &+2(\mathbf{u}_r^{(i)}[n]-\mathbf{u}_e[n])\cdot(\mathbf{u}_r[n]-\mathbf{u}_r^{(i)}[n]) \ge d_{\min}^2, \forall k,n.\end{aligned} \tag{40}$$

$$\theta_{1,k}[n] \le f_{1,\mathrm{T}}(\mathbf{u}_r[n]) - f_{2,\mathrm{T}}(\mathbf{u}_r[n]), \forall k,n, \tag{41}$$

where $f_{\alpha,\mathrm{T}}(\mathbf{u}_r[n]), \alpha\in\{1,2\}$, can be written as (42), where $f_\alpha(\mathbf{u}_r^{(i)}[n])$ can be written as

$$f_\alpha(\mathbf{u}_r^{(i)}[n]) = \log_2\left(g_\alpha(\mathbf{u}_r^{(i)}[n])\right), \forall k,n, \tag{43}$$

where $g_1(\mathbf{u}_r^{(i)}[n])$ and $g_2(\mathbf{u}_r^{(i)}[n])$ are written as (44a) and (44b), and $\nabla g_1(\mathbf{u}_r^{(i)}[n])$ and $\nabla g_2(\mathbf{u}_r^{(i)}[n])$ can be written as (45a) and (45b), where

$$a_{u_1,u_2}[n] = \left(\sqrt{\frac{\widetilde{G}[n]}{\widetilde{G}[n]+1}}+\sqrt{\frac{1}{\widetilde{G}[n]+1}}\widetilde{g}_{u_1,u_2}[n]\right)^4, \tag{46}$$

where $(u_1,u_2)\in\{(k,r),(s,r),(j,r)\}$.

Then, the problem (P4) can be reformulated as

$$\text{(P4.1)}: \max_{\{\mathbf{u}_r[n],\theta_{1,k}[n],\theta_{2,k}[n]\}} \theta \quad \text{s.t. (1),(25b),(25d)-(25f),(40),(41).} \tag{47}$$

Note that (P4.1) is typically convex, which can be solved by CVX.

The original problem (P1) can be solved by iteratively solving the problems (P3) and (P4) to approach the global optimal solution, in which the variables are optimized by updating in an alternating manner as shown in Algorithm 1.

Algorithm 1 BCD-Based Joint Optimization Algorithm

1: **Init:** $\mathcal{V}^{(0)}[n]=\{\xi_k^{(0)}[n],p_k^{(0)}[n],p_r^{(0)}[n],l_{k,\mathrm{loc}}^{(0)}[n],\mathbf{u}_r^{(0)}[n]\}$, set $\varepsilon>0$.
2: **repeat**
3: By $\mathcal{V}^{(i)}[n]\backslash\xi_k^{(i)}[n]$, solve the problem (P3.1), obtain and update time allocation $\xi_k[n]$.
4: By $\mathcal{V}^{(i)}[n]\backslash p_k^{(i)}[n]$, solve the problem (P3.2), obtain and update MD$_k$ transmit power $p_k[n]$.
5: By $\mathcal{V}^{(i)}[n]\backslash p_r^{(i)}[n]$, solve the problem (P3.3), obtain and update UAV$_r$ transmit power $p_r[n]$.
6: By $\mathcal{V}^{(i)}[n]\backslash l_{k,\mathrm{loc}}^{(i)}[n]$, solve the problem (P3.4), obtain and update MD$_k$ local computation allocation $l_{k,\mathrm{loc}}[n]$.
7: By $\mathcal{V}^{(i)}[n]\backslash\mathbf{u}_r^{(i)}[n]$, solve the problem (P4), obtain and update UAV$_r$ trajectory $\mathbf{u}_r[n]$.
8: Update $i\leftarrow i+1$.
9: **until** The accuracy ε is achieved or i reaches I_1.
10: **Output:** $\xi_k[n]$, $p_k[n]$, $p_r[n]$, $l_{k,\mathrm{loc}}[n]$, $\mathbf{u}_r[n]$.

C. Feasibility and Complexity of Algorithm 1

The required Q_k may not satisfy the initialization parameters on the initial iteration. To make the problem solvable, we

$$f_{\alpha,\mathrm{T}}(\mathbf{u}_r[n]) = f_\alpha\left(\mathbf{u}_r^{(i)}[n]\right) + \nabla f_\alpha\left(\mathbf{u}_r^{(i)}[n]\right)\left(\mathbf{u}_r[n] - \mathbf{u}_r^{(i)}[n]\right) = f_\alpha\left(\mathbf{u}_r^{(i)}[n]\right) + \frac{\nabla g_\alpha\left(\mathbf{u}_r^{(i)}[n]\right)}{g_\alpha\left(\mathbf{u}_r^{(i)}[n]\right)\ln 2}\left(\mathbf{u}_r[n] - \mathbf{u}_r^{(i)}[n]\right), \forall k, n, \quad (42)$$

$$\begin{aligned} g_1(\mathbf{u}_r^{(i)}[n]) &= n_r^2 n_s^2 d_{j,r}^2[n] d_{k,r}^2[n] d_{r,s}^2[n] + a_{j,r}[n] n_s^2 P_j \beta_0 d_{k,r}^2[n] d_{r,s}^2[n] + a_{k,r}[n] n_s^2 p_k[n] \beta_0 d_{j,r}^2[n] d_{r,s}^2[n] \\ &\quad + a_{r,s}[n] n_r^2 p_r[n] \beta_0 d_{j,r}^2[n] d_{k,r}^2[n] + a_{k,r}[n] a_{r,s}[n] p_k[n] p_r[n] \beta_0^2 d_{j,r}^2[n], \forall k, n, \quad (44a) \\ g_2(\mathbf{u}_r^{(i)}[n]) &= n_r^2 n_s^2 d_{j,r}^2[n] d_{k,r}^2[n] d_{r,s}^2[n] + a_{j,r}[n] n_s^2 P_j \beta_0 d_{k,r}^2[n] d_{r,s}^2[n] + a_{k,r}[n] n_s^2 p_k[n] \beta_0 d_{j,r}^2[n] d_{r,s}^2[n] \\ &\quad + a_{r,s}[n] n_r^2 p_r[n] \beta_0 d_{j,r}^2[n] d_{k,r}^2[n], \forall k, n. \quad (44b) \end{aligned}$$

$$\begin{aligned} \nabla g_1(\mathbf{u}_r^{(i)}[n]) &= 2 n_r^2 n_s^2 \left((\mathbf{u}_r^{(i)}[n] - \mathbf{v}_j) d_{k,r}^2[n] d_{r,s}^2[n] + d_{j,r}^2[n] (\mathbf{u}_r^{(i)}[n] - \mathbf{v}_k) d_{r,s}^2[n] + d_{j,r}^2[n] d_{k,r}^2[n] (\mathbf{u}_r^{(i)}[n] - \mathbf{v}_s) \right) \\ &\quad + 2 a_{j,r}[n] n_s^2 P_j \beta_0 \left((\mathbf{u}_r^{(i)}[n] - \mathbf{v}_k) d_{r,s}^2[n] + d_{k,r}^2[n] (\mathbf{u}_r^{(i)}[n] - \mathbf{v}_s) \right) \\ &\quad + 2 a_{k,r}[n] n_s^2 p_k[n] \beta_0 \left((\mathbf{u}_r^{(i)}[n] - \mathbf{v}_j) d_{r,s}^2[n] + d_{j,r}^2[n] (\mathbf{u}_r^{(i)}[n] - \mathbf{v}_s) \right) \\ &\quad + 2 a_{r,s}[n] n_r^2 p_r[n] \beta_0 \left((\mathbf{u}_r^{(i)}[n] - \mathbf{v}_j) d_{k,r}^2[n] + d_{j,r}^2[n] (\mathbf{u}_r^{(i)}[n] - \mathbf{v}_k) \right) \\ &\quad + 2 a_{k,r}[n] a_{r,s}[n] p_k[n] p_r[n] \beta_0^2 (\mathbf{u}_r^{(i)}[n] - \mathbf{v}_j), \forall k, n, \quad (45a) \\ \nabla g_2(\mathbf{u}_r^{(i)}[n]) &= 2 n_r^2 n_s^2 \left((\mathbf{u}_r^{(i)}[n] - \mathbf{v}_j) d_{k,r}^2[n] d_{r,s}^2[n] + d_{j,r}^2[n] (\mathbf{u}_r^{(i)}[n] - \mathbf{v}_k) d_{r,s}^2[n] + d_{j,r}^2[n] d_{k,r}^2[n] (\mathbf{u}_r^{(i)}[n] - \mathbf{v}_s) \right) \\ &\quad + 2 a_{j,r}[n] n_s^2 P_j \beta_0 \left((\mathbf{u}_r^{(i)}[n] - \mathbf{v}_k) d_{r,s}^2[n] + d_{k,r}^2[n] (\mathbf{u}_r^{(i)}[n] - \mathbf{v}_s) \right) \\ &\quad + 2 a_{k,r}[n] n_s^2 p_k[n] \beta_0 \left((\mathbf{u}_r^{(i)}[n] - \mathbf{v}_j) d_{r,s}^2[n] + d_{j,r}^2[n] (\mathbf{u}_r^{(i)}[n] - \mathbf{v}_s) \right) \\ &\quad + 2 a_{r,s}[n] n_r^2 p_r[n] \beta_0 \left((\mathbf{u}_r^{(i)}[n] - \mathbf{v}_j) d_{k,r}^2[n] + d_{j,r}^2[n] (\mathbf{u}_r^{(i)}[n] - \mathbf{v}_k) \right), \forall k, n. \quad (45b) \end{aligned}$$

first check the feasibility of Algorithm 1 by optimizing the problem as

$$\begin{aligned} (\mathrm{P5}): \max_{\{\xi_k[n], p_k[n], p_r[n], l_{k,\mathrm{loc}}[n], \mathbf{u}_r[n]\}} & Q_k^u \quad (48a) \\ \text{s.t. } & (1),(2),(5),(6),(17),(18),(22), \\ & l_{k,\mathrm{loc}}[n] + \frac{1}{2} W \xi_k[n] \varphi_t \Phi_{k,\mathrm{sec}} \geq Q_k^u, \forall k, n. \quad (48b) \end{aligned}$$

Through solving the problem (P5), we can obtain Q_k^u. Subsequently, we can assess the feasibility of Algorithm 1 and adjust the parameter initialization accordingly to ensure better performance [29].

In each iteration of the proposed algorithm, there are two standard convex optimization solutions and three S-CA techniques, and the number of variables involved is $4KN + N$. Taking I_1 as the iteration number of BCD algorithm, we have the complexity of Algorithm 1 given as $I_1 O((KN)^{3.5} \log(1/\varepsilon))$ [37].

TABLE II
PARAMETER SETTING

Parameters	Values
Channel power gain at a unit distance	$\beta_0 = -60$ dB
Altitude of UAVs	$H_r = H_e = 100$ m
The power ratio of signal matrix	$\widetilde{G}[n] = 30$
Length of the time slot	$\varphi_t = 0.5$ s
Received noise power	$n_r = n_e = n_s = -110$ dBm
CPU cycles required per bit computing	$c_k = c_s = 10^3$ cycles/bit
Maximum CPU frequency	$F_k^{\max} = 10^9$ Hz, $F_s^{\max} = 10^{12}$ Hz
Communication bandwidth	$W = 1$ MHz
MD_k CPU capacity coefficient	$k_k = 10^{-27}$
MD_k power budget	$P_k^{\mathrm{ave}} = 1$ W

V. NUMERICAL RESULTS

In this section, we first evaluate the convergence of the proposed algorithm. Then, the impact of different constraints on the max-min secure computing capacity is compared. Lastly, we conduct a comparison between the proposed algorithm and four benchmark approaches. Some parameters are provided in Table II, and others are as follows [5], [31].

Within a sea area of 1500×2000 m^2, we deploy five MDs

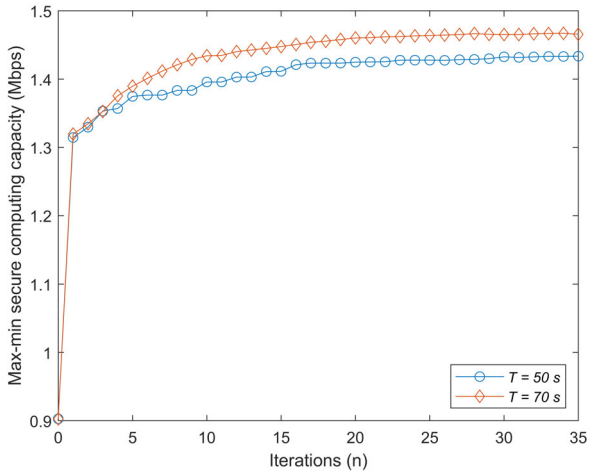

Fig. 2. Convergence of Algorithm 1 with different values of T, where $P_k^{\max} = 0.2$ W, $P_r^{\max} = 0.5$ W and $P_j = 0.5$ W.

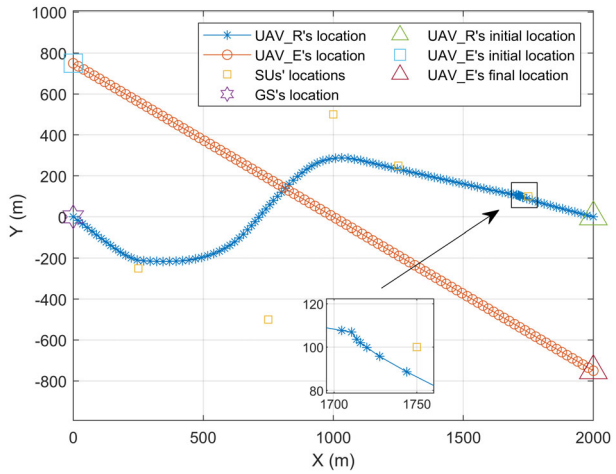

Fig. 3. Optimized trajectories for UAV$_r$ vs. T, where $P_k^{\max} = 0.1$ W, $P_r^{\max} = 0.5$ W, $P_j = 0.5$ W, and $T = 50$ s.

in our proposed scheme. The locations of CES and CJ are both fixed at $[0, 0]^T$. UAV$_r$ flies from $\mathbf{u}_r^I = [0, 0]^T$ to $\mathbf{u}_r^F = [2000, 0]^T$, and UAV$_e$ flies from $\mathbf{u}_e^I = [0, 750]^T$ to $\mathbf{u}_e^F = [2000, -750]^T$, in meters. The maximum speed of UAV$_r$ is set as $V_r^{\max} = 50$ m/s. The minimum collision avoidance distance between UAVs is set as $d_{\min} = 1$ m. UAV$_e$ flies along a straight line with a constant speed.

Fig. 2 shows the convergence of our proposed algorithm while considering different values of T. In Fig. 2, it becomes apparent that an increase in the value of T results in a corresponding increase in the max-min secure computing capacity. This occurrence can be attributed to the fact that as T grows larger, the UAV$_r$ can be afforded more time to approach the MDs, enabling it to deliver improved service quality. The extended duration allows the UAV$_r$ to establish closer proximity with the MDs. Thus, enhancing the overall performance and contributing to the higher secure computing capacity.

Fig. 3 and Fig. 4 show the optimized trajectories of UAV$_r$ in our proposed scheme with different T. Meanwhile, the given trajectory of UAV$_e$ is also shown. In the case of $T = 50$ s as shown in Fig. 3, because of the short time, UAV$_r$ almost passes over a few MDs during the flight. With longer time $T = 70$ s as shown in Fig. 4, UAV$_r$ can pass over more MDs, obtaining more time slots staying above each MD. Thus, the hovering time over each MD will be longer, resulting in better performance as illustrated in Fig. 6 and Fig. 7.

Fig. 5 illustrates the optimized speeds for UAV$_r$ with different T. As shown in Fig. 3 and Fig. 4, UAV$_r$ will pass over as many MDs as possible, and hover over each MD as long as possible. It results that UAV$_r$ flies away from a MD as fast as possible, and slows down slowly when it approaches next MD. As shown in Fig. 5(a), there is a significant change in the speed of UAV$_r$ between time slot 80 and 90, indicating that UAV$_r$ stays above the corresponding MD for a longer period of time. And in Fig. 5(b), a similar change in speed occurs five times. It can be seen that UAV$_r$ has more time to approach MDs to provide better service due to the increase T.

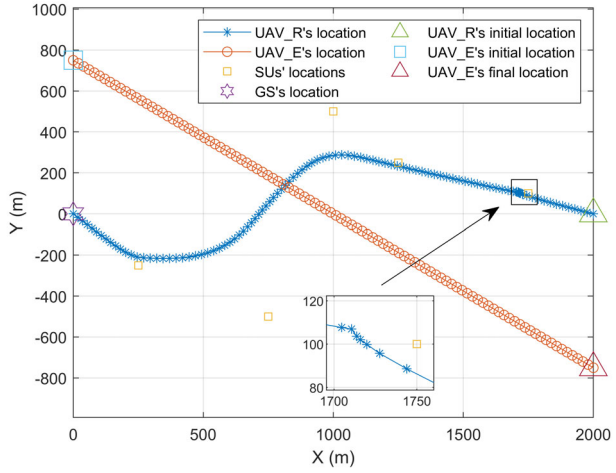

Fig. 4. Optimized trajectories for UAV$_r$ vs. T, where $P_k^{\max} = 0.1$ W, $P_r^{\max} = 0.5$ W, $P_j = 0.5$ W, and $T = 70$ s.

Fig. 6 illustrates the max-min secure computing capacity with different values of $P_k^{\max}$. It can be observed that with the increase of $P_k^{\max}$, the max-min secure computing capacity is becoming larger. This is because with higher transmit power, MDs will have more energy to offload computing tasks to CES through UAV$_r$, which has more powerful computing ability.

Fig. 7 shows the max-min secure computing capacity with different values of $P_r^{\max}$. When $P_r^{\max}$ becomes larger, UAV$_r$ can forward more information to CES with larger information rate. While CJ only transmits the jamming signal in the first phase of each time slot. Thus, for the information forwarded by UAV$_r$ to CES, the effective transmission rate increases with larger $P_r^{\max}$, resulting in a better performance.

Fig. 8 shows the max-min secure computing capacity with different values of P_j. It can be observed that with increase of P_j, the max-min secure computing capacity is becoming larger. This is because CES knows the interference signal emitted by CJ in advance, while UAV$_e$ does not. When

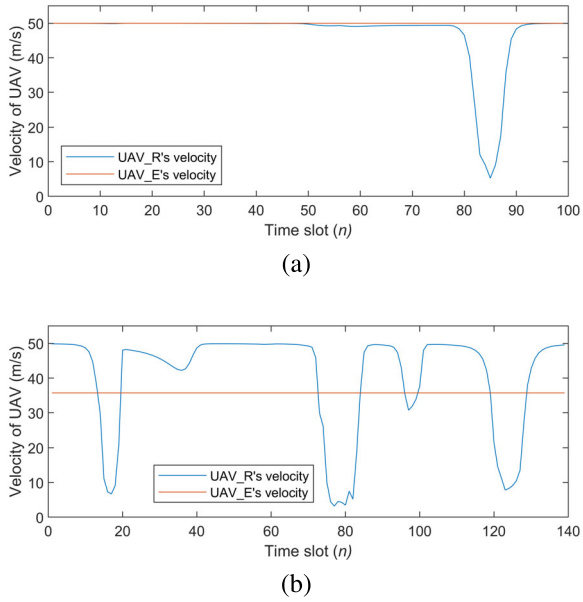

Fig. 5. Optimized flight speeds for UAV$_r$ with different T, where $P_k^{\max} = 0.1$ W, $P_r^{\max} = 0.5$ W and $P_j = 0.5$ W. (a) $T = 50$ s, (b) $T = 70$ s.

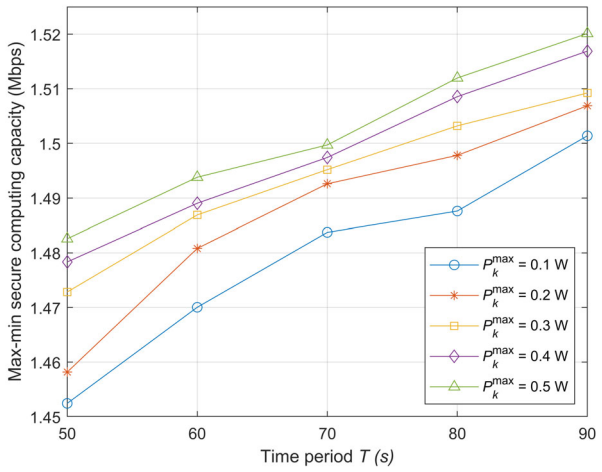

Fig. 6. Secure computing capacity with different $P_k^{\max}$, where $P_r^{\max} = 0.8$ W and $P_j = 0.5$ W.

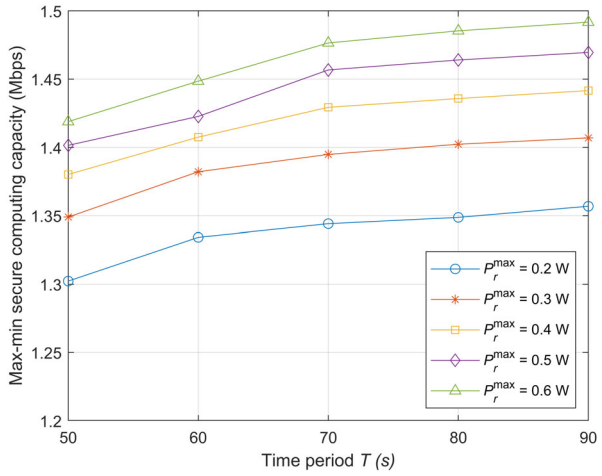

Fig. 7. Secure computing capacity with different $P_r^{\max}$, where $P_k^{\max} = 0.1$ W and $P_j = 0.5$ W.

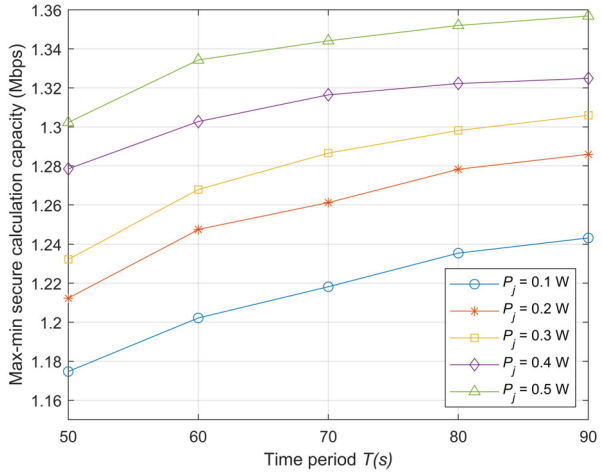

Fig. 8. Secure computing capacity with different P_j, where $P_k^{\max} = 0.1$ W and $P_r^{\max} = 0.2$ W.

P_j increases, producing stronger interference to the UAV$_e$, resulting in a smaller eavesdropping rate.

Fig. 9 and Fig. 10 illustrate the secure computing capacity comparisons of our proposed algorithm with four benchmarks with the same target of maximizing secure computing capacity of the system. The specific descriptions of four benchmarks are as follows.

Algorithm 2: The time slot allocation factor $\xi_k[n]$ is fixed, while MD$_k$ transmit power $p_k[n]$, UAV$_r$ transmit power $p_r[n]$, MD$_k$ local computation allocation $l_{k,\mathrm{loc}}[n]$, and UAV$_r$ trajectory $\mathbf{u}_r[n]$ are optimized.

Algorithm 3: MD$_k$ transmit power $p_k[n]$ is fixed, while the time slot allocation factor $\xi_k[n]$, MD$_k$ local computation allocation $l_{k,\mathrm{loc}}[n]$, UAV$_r$ transmit power $p_r[n]$, and UAV$_r$ trajectory $\mathbf{u}_r[n]$ are optimized.

Algorithm 4: UAV$_r$ transmit power $p_r[n]$ is fixed, while the time slot allocation factor $\xi_k[n]$, MD$_k$ local computation allocation $l_{k,\mathrm{loc}}[n]$, MD$_k$ transmit power $p_k[n]$, and UAV$_r$ trajectory $\mathbf{u}_r[n]$ are optimized.

Algorithm 5: UAV$_r$ trajectory $\mathbf{u}_r[n]$ is fixed, while the time slot allocation factor $\xi_k[n]$, MD$_k$ local computation allocation $l_{k,\mathrm{loc}}[n]$, MD$_k$ transmit power $p_k[n]$, and UAV$_r$ transmit power $p_r[n]$ are optimized.

By comparing the secure computing capacity of the proposed algorithm with four benchmarks having different $P_k^{\max}$ values in Fig. 9, it is evident that the proposed algorithm is better. The proposed algorithm outperforms four benchmarks with different values of $P_k^{\max}$. Furthermore, the proposed algorithm optimizes the time slot allocation factor when it is compared to Algorithm 2, highlighting the importance of this factor in improving performance. In addition to optimizing the transmit power of MD$_k$, the proposed algorithm significantly improves performance compared to Algorithm 3. Furthermore, the proposed algorithm optimizes the transmit power of UAV$_r$ to enhance performance, a factor not considered in Algorithm

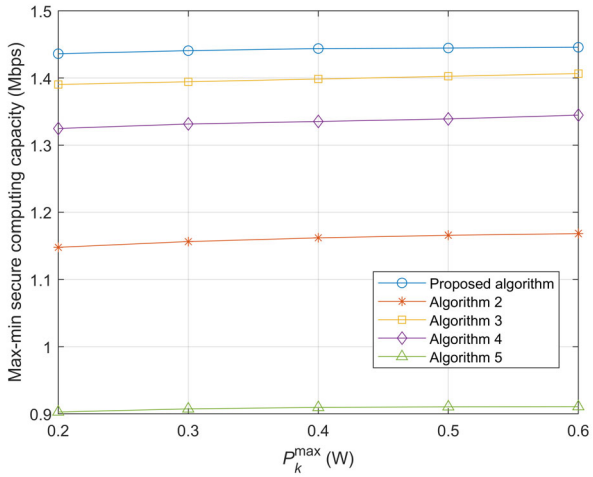

Fig. 9. Secure computing capacity with different $P_k^{\max}$, where $T = 50$ s, $P_r^{\max} = 0.5$ W and $P_j = 0.5$ W. Algorithm 2 - 5 are four benchmarks.

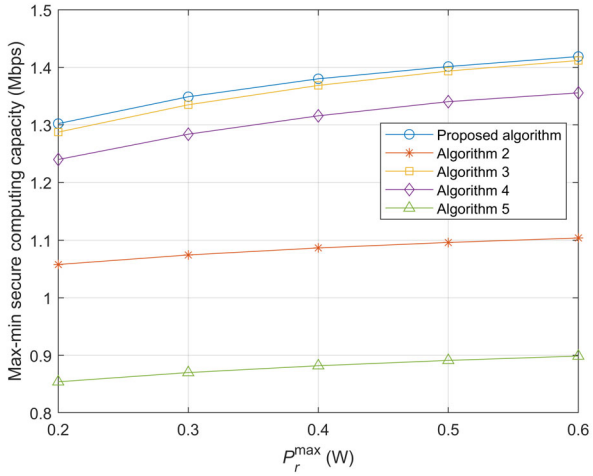

Fig. 10. Secure computing capacity with different $P_r^{\max}$, where $T = 50$ s, $P_k^{\max} = 0.1$ W and $P_j = 0.5$ W. Algorithm 2 - 5 are four benchmarks.

4. Finally, compared to Algorithm 5, the proposed algorithm also optimizes the UAV$_r$ trajectory, indicating the significance of this factor in improving performance.

In Fig. 10, it is evident that the proposed algorithm outperforms four benchmarks with different values of $P_r^{\max}$. It can be observed that Algorithm 2 achieves a lower performance in secure offloading rate as it does not optimize the time slot allocation factor. Similarly, Algorithm 3 achieves a lower performance in secure offloading rate as it does not optimize MD$_k$ transmit power. Algorithm 4 achieves a lower performance in secure offloading rate as it does not optimize UAV$_r$ transmit power. Finally, Algorithm 5 achieves a lower performance in secure offloading rate as it does not optimize UAV$_r$ trajectory. This highlights the significance of optimizing time slot allocation factor, MD$_k$ and UAV$_r$ transmit powers, and UAV$_r$ trajectory in enhancing the overall performance of the proposed algorithm.

VI. Conclusion

In this paper, a secure communication scheme was proposed to enhance the secure computing capacity performance for the UAV-relay-assisted maritime MEC, where UAV$_r$ helps to forward the offloading tasks of MDs to CES. To reduce UAV$_e$ eavesdropping, CJ generates the interfering signals. The max-min secure computing capacity of MDs is achieved by optimizing the UAV trajectory, time slot allocation, transmit power and computation allocation with the constraints of UAV$_r$ flight speed, UAV anti-collision, UAV$_r$ transmit power, MDs transmit power, MDs local computation ability, MDs computing task requirements and CES CPU frequency. The formulated OP is non-convexity because of the coupling of multiple variables. We first transform OP by introducing auxiliary variables. Then, the transformed OP is decomposed and solved in an iterative manner by applying BCD and SCA. The simulation results show that the proposed algorithm can achieve better secure computing capacity performance compared with four benchmarks.

References

[1] T. Xia, M. M. Wang, J. Zhang and L. Wang, Maritime internet of things: Challenges and solutions, *IEEE Wireless Commun.*, vol. 27, no. 2, pp. 188-196, Apr. 2020.

[2] Y. Li, Y. Zhang, W. Li and T. Jiang, Marine wireless big data: Efficient transmission, related applications, and challenges, *IEEE Wireless Commun.*, vol. 25, no. 1, pp. 19-25, Feb. 2018.

[3] Y. Mao, C. You, J. Zhang, K. Huang and K. B. Letaief, A survey on mobile edge computing: The communication perspective, *IEEE Commun. Surveys Tuts.*, vol. 19, no. 4, pp. 2322-2358, Aug. 2017.

[4] M. Mozaffari, X. Lin and S. Hayes, Toward 6G with connected sky: UAVs and beyond, *IEEE Commun. Mag.*, vol. 59, no. 12, pp. 74-80, Dec. 2021.

[5] T. Zhang, Y. Xu, J. Loo, D. Yang and L. Xiao, "Joint computation and communication design for UAV-assisted mobile edge computing in IoT," *IEEE Trans. Ind. Informat.*, vol. 16, no. 8, pp. 5505-5516, Aug. 2020.

[6] A. Fotouhi, H. Qiang, M. Ding, M. Hassan, L. G. Giordano, A. Garcia-Rodriguez and J. Yuan, Survey on UAV cellular communications: Practical aspects, standardization advancements, regulation, and security challenges, *IEEE Commun. Surveys Tuts.*, vol. 21, no. 4, pp. 3417-3442, Mar. 2019.

[7] Y. Zeng, R. Zhang and T. J. Lim, Throughput maximization for UAV-enabled mobile relaying systems, *IEEE Trans. Commun.*, vol. 64, no. 12, pp. 4983-4996, Dec. 2016.

[8] Y. Chen, N. Zhao, Z. Ding and M.-S. Alouini, Multiple UAVs as relays: Multi-hop single link versus multiple dual-hop links, *IEEE Trans. Wireless Commun.*, vol. 17, no. 9, pp. 6348-6359, Sept. 2018.

[9] N. Zhao, W. Lu, M. Sheng, Y. Chen, J. Tang, F. R. Yu and K.-K. Wong, UAV-assisted emergency networks in disasters, *IEEE Wireless Commun.*, vol. 26, no. 1, pp. 45-51, Feb. 2019.

[10] X. Zhong, Y. Guo, N. Li and Y. Chen, Joint optimization of relay deployment, channel allocation, and relay assignment for UAVs-aided D2D networks, *IEEE/ACM Trans. Netw.*, vol. 28, no. 2, pp. 804-817, Apr. 2020.

[11] Y. Liang, L. Xiao, D. Yang, Y. Liu and T. Zhang, Joint trajectory and resource optimization for UAV-aided two-way relay networks, *IEEE Trans. Veh. Technol.*, vol. 71, no. 1, pp. 639-652, Jan. 2022.

[12] J. Zhang, F. Liang, B. Li, Z. Yang, Y. Wu and H. Zhu, Placement optimization of caching UAV-assisted mobile relay maritime communication, *China Commun.*, vol. 17, no. 8, pp. 209-219, Aug. 2020.

[13] C. Zhan, H. Hu, X. Sui, Z. Liu and D. Niyato, "Completion time and energy optimization in the UAV-enabled mobile-edge computing system," *IEEE Internet Things J.*, vol. 7, no. 8, pp. 7808-7822, Aug. 2020.

[14] F. Zhou, R. Q. Hu, Z. Li and Y. Wang, Mobile edge computing in unmanned aerial vehicle networks, *IEEE Wireless Commun.*, vol. 27, no. 1, pp. 140-146, Feb. 2020.

[15] Q. Hu, Y. Cai, G. Yu, Z. Qin, M. Zhao and G. Y. Li, Joint offloading and trajectory design for UAV-enabled mobile edge computing systems, *IEEE Internet Things J.*, vol. 6, no. 2, pp. 1879-1892, Apr. 2019.
[16] X. Hu, K.-K. Wong, K. Yang and Z. Zheng, UAV-assisted relaying and edge computing: Scheduling and trajectory optimization, *IEEE Trans. Wireless Commun.*, vol. 18, no. 10, pp. 4738-4752, Oct. 2019.
[17] L. Guo, X. Ji and S. Zhang, "Energy-efficient full-duplex UAV relaying with trajectory optimization and power control in maritime communication environments," *China Commun.*, vol. 19, no. 12, pp. 216-231, Dec. 2022.
[18] Z. Na, C. Ji, B. Lin and N. Zhang, "Joint optimization of trajectory and resource allocation in secure UAV relaying communications for internet of things," *IEEE Internet Things J.*, vol. 9, no. 17, pp. 16284-16296, 1 Sept.1, 2022.
[19] L. Zhang and N. Ansari, Optimizing the operation cost for UAV-aided mobile edge computing, *IEEE Trans. Veh. Technol.*, vol. 70, no. 6, pp. 6085-6093, Jun. 2021.
[20] B. Liu, Y. Wan, F. Zhou, Q. Wu and R. Q. Hu, Resource allocation and trajectory design for MISO UAV-assisted MEC networks, *IEEE Trans. Veh. Technol.*, vol. 71, no. 5, pp. 4933-4948, May 2022.
[21] X. He, R. Jin and H. Dai, Multi-hop task offloading with on-the-fly computation for multi-UAV remote edge computing, *IEEE Trans. Commun.*, vol. 70, no. 2, Feb. 2022.
[22] L. Zhao, K. Yang, Z. Tan, X. Li, S. Sharma and Z. Liu, A novel cost optimization strategy for SDN-enabled UAV-assisted vehicular computation offloading, *IEEE Trans. Intell. Transp. Syst.*, vol. 22, no. 6, pp. 3664-3674, Jun. 2021.
[23] B. Li, Z. Fei, Y. Zhang and M. Guizani, Secure UAV communication networks over 5G, *IEEE Wireless Commun.*, vol. 26, no. 5, pp. 114-120, Oct. 2019.
[24] Y. Liu, H.-H. Chen and L. Wang, Physical layer security for next generation wireless networks: Theories, technologies, and challenges, *IEEE Commun. Surveys Tuts.*, vol. 19, no. 1, pp. 347-376, Aug. 2017.
[25] D. Wang, B. Bai, W. Zhao and Z. Han, A survey of optimization approaches for wireless physical layer security, *IEEE Commun. Surveys Tuts.*, vol. 21, no. 2, pp. 1878-1911, Nov. 2019.
[26] Q. Wang, Z. Chen, W. Mei and J. Fang, Improving physical layer security using UAV-enabled mobile relaying, *IEEE Wireless Commun. Lett.*, vol. 6, no. 3, pp. 310-313, Jun. 2017.
[27] Y. Zhou, C. Pan, P. L. Yeoh, K. Wang, M. Elkashlan, B. Vucetic and Y. Li, Secure communications for UAV-enabled mobile edge computing systems, *IEEE Trans. Commun.*, vol. 68, no. 1, pp. 376-388, Jan. 2020.
[28] Y. Li, Y. Fang and L. Qiu, Joint computation offloading and communication design for secure UAV-enabled MEC systems, in *Proc. IEEE Wireless Commun. Netw. Conf. (WCNC)*, Nanjing, China, Mar. 2021, pp. 1-6.
[29] Y. Xu, T. Zhang, D. Yang, Y. Liu and M. Tao, Joint resource and trajectory optimization for security in UAV-assisted MEC systems, *IEEE Trans. Commun.*, vol. 69, no. 1, pp. 573-588, Jan. 2021.
[30] W. Lu, Y. Ding, Y. Gao, S. Hu, Y. Wu, N. Zhao and Y. Gong, Resource and trajectory optimization for secure communications in dual unmanned aerial vehicle mobile edge computing systems, *IEEE Trans. Ind. Informat.*, vol. 18, no. 4, pp. 2704-2713, Apr. 2022.
[31] W. Lu, Y. Ding, Y. Gao, Y. Chen, N. Zhao, Z. Ding and A. Nallanathan, Secure NOMA-based UAV-MEC network towards a flying eavesdropper, *IEEE Trans. Commun.*, vol. 70, no. 5, pp. 3364-3376, May 2022.
[32] W. Wang, X. Li, R. Wang, K. Cumanan, W. Feng, Z. Ding and O. A. Dobre, Robust 3D-trajectory and time switching optimization for dual-UAV-enabled secure communications, *IEEE J. Sel. Areas Commun.*, vol. 39, no. 11, pp. 3334-3347, Nov. 2021.
[33] *Enhanced LTE support for aerial vehicles.* Accessed: Jul. 16, 2017. [Online]. Available:ftp://www.3gpp.org/specs/archive/36_series/36.777.
[34] P. Tseng, Convergence of a block coordinate descent method for nondifferentiable minimization, *J. Optim. Theory Appl.*, vol. 109, pp. 475-494, 2001.
[35] S. P. Boyd and L. Vandenberghe, *Convex Optimization.* Cambridge, U.K.: Cambridge Univ. Press, 2004.
[36] B. R. Marks and G. P. Wright, A general inner approximation algorithm for nonconvex mathematical programs, *Oper. Res.*, vol. 26, no. 4, pp. 681-683, 1978.
[37] M. Li, N. Cheng, J. Gao, Y. Wang, L. Zhao and X. Shen, Energy-efficient UAV-assisted mobile edge computing: Resource allocation and trajectory optimization, *IEEE Trans. Veh. Technol.*, vol. 69, no. 3, pp. 3424-3438, Mar. 2020.

Resource and Trajectory Optimization for UAV-Relay-Assisted Secure Maritime MEC

Fangwei Lu, Gongliang Liu, Weidang Lu, *Senior Member, IEEE*,
Yuan Gao, Jiang Cao, Nan Zhao, *Senior Member, IEEE*,
Arumugam Nallanathan, *Fellow, IEEE*

Abstract

With the evolutional development of maritime networks, the explosive growth of maritime data has put forward elevated demands for the computing capabilities of maritime devices (MDs). Unmanned aerial vehicle (UAV) is able to alleviate the computing pressure of MDs by forwarding the computing tasks to the edge server on the coast. However, UAV relaying introduces a significant security challenge due to the vulnerability of line-of-sight (LoS) communication channels, which can be exploited for eavesdropping on computing tasks. In this paper, an efficient secure communication scheme is proposed for UAV-relay-assisted maritime mobile edge computing (MEC) with a flying eavesdropper. The secure computing capacity of MDs is maximized by jointly optimizing the transmit power, time slot allocation factor, computation optimization and UAV trajectory. Due to multi-variable coupling, the formulated optimization problem (OP) is non-convex. We first transform OP by introducing auxiliary variables. Then, the transformed OP is decomposed and solved in an iterative manner by applying block coordinate descent (BCD) and successive convex approximation (SCA). Numerical results show

Fangwei Lu and Gongliang Liu are with the Department of Communication Engineering, Harbin Institute of Technology, Weihai 264209, China (e-mail: lufangwei2022@163.com; liugl@hit.edu.cn).

Weidang Lu is with the College of Information Engineering, Zhejiang University of Technology, Hangzhou 310023, China (e-mail: luweid@zjut.edu.cn).

Yuan Gao and Jiang Cao are with the Academy of Military Science of the PLA, China (e-mail: yuangao08@tsinghua.edu.cn; caojiangjk@outlook.com).

Nan Zhao is with the School of Information and Communication Engineering, Dalian University of Technology, Dalian 116024, P. R. China (e-mail: zhaonan@dlut.edu.cn).

Arumugam Nallanathan is with School of Electronic Engineering and Computer Science, Queen Mary University of London, E1 4NS, U.K. (e-mail: a.nallanathan@qmul.ac.uk).